




# Surface modification of zirconia dental implants by laser texturing

Welson Cunha<sup>1</sup> · Oscar Carvalho<sup>2</sup> · Bruno Henriques<sup>2,3</sup> · Filipe S. Silva<sup>2</sup> · Mutlu Özcan<sup>4</sup> · Júlio C. M. Souza<sup>1,2</sup> 

Received: 20 January 2021 / Accepted: 16 November 2021 / Published online: 13 January 2022  
© The Author(s), under exclusive licence to Springer-Verlag London Ltd., part of Springer Nature 2021

## Abstract

The aim of this work was to perform an integrative literature review on the influence of laser irradiation on zirconia implants to enhance surface topographic aspects and the biological response for osseointegration. An electronic search was carried out on the PubMed database using the following search terms: “zirconia” AND “laser” AND “surface modification” OR “surface treatment” AND “dental implants” OR “bone” OR “osteoblast” OR “osseointegration.” Of the identified articles, 12 studies were selected in this review. Results reported that the laser irradiation was capable of promoting changes on the zirconia surfaces regarding topographic aspects, roughness, and wettability. An increase in roughness was recorded at micro- and nano-scale and it resulted in an enhanced wettability and biological response. Also, adhesion, spreading, proliferation, and differentiation of osteogenic cells were also enhanced after laser irradiation mainly by using a femtosecond laser at 10nJ and 80 MHz. After 3 months of osseointegration, *in vivo* studies in dogs revealed a similar average percentage of bone-to-implant contact (BIC) on zirconia surfaces (around  $47.9 \pm 16\%$ ) when compared to standard titanium surfaces ( $61.73 \pm 16.27\%$ ), denoting that there is no significant difference between such different materials. The laser approach revealed several parameters that can be used for zirconia surface modification such as irradiation intensity, time, and frequency. Laser irradiation parameters can be optimized and well-controlled to reach desirable surface morphologic aspects and biological response concerning the osseointegration process.

**Keywords** Zirconia · Surface treatment · Laser · Dental implants · Osseointegration

## Introduction

In implant dentistry, osseointegration has been studied considering the direct, structural, and functional connection between bone tissue and implant surfaces over occlusal loading [1–4]. The long-term stability of dental implants depends on the chemical composition and surface of

implants materials; although, the health state of patients also affect osseointegration [5, 6]. On standard titanium dental implants, several physicochemical techniques have been successfully used for enhanced osseointegration such as double acidic etching and grit-blasting [3, 6]. However, the surface modification of zirconia surfaces revealed different outcomes taking into consideration ordinary physicochemical techniques [7–11]. At first, the surface topographic aspects are quite different when compared to those noticed on titanium surfaces [8, 11, 12]. Second, the ordinary acidic etching has no effect on zirconia surfaces regarding roughness changes [11]. In this way, advanced surface modification methods have been developed to modify zirconia surfaces and maintaining the physical performance of the material [12–17].

Zirconia is a chemically stable and biocompatible ceramic material that has been used for implants and prosthetics in orthopedics and dentistry [5, 18–20]. The chemical stability of zirconia becomes a challenge concerning the surface modification [11, 19]. The physical properties of zirconia are achieved by stabilizing the tetragonal zirconia phase

✉ Júlio C. M. Souza  
jsouza@dem.uminho.pt

<sup>1</sup> School of Dentistry, University Institute of Health Sciences (IUCS), CESPU, 4585-116 Gandra PRD, Portugal

<sup>2</sup> Center for MicroElectroMechanical Systems (CMEMS-UMINHO), University of Minho, Campus Azurém, 4800-058 Guimarães, Portugal

<sup>3</sup> Ceramic and Composite Materials Research Group (CERMAT), Dept. of Mechanical Engineering (EMC), Federal University of Santa Catarina (UFSC), Florianópolis 88040-900, Brazil

<sup>4</sup> Division of Dental Biomaterials, Clinic for Reconstructive Dentistry, Center of Dental Medicine, University of Zürich, Zürich 8032, Switzerland

at room temperature by incorporating small contents of different oxides, namely  $Y_2O_3$ , MgO,  $CeO_2$ , or CaO [21, 18]. For instance, yttria-stabilized tetragonal zirconia polycrystals (Y-TZP) has a flexural strength at 900–1200 MPa, elastic modulus of approximately 210 GPa, and fracture toughness at around 7–10  $MPa \cdot m^{1/2}$  [20, 18]. In vitro and in vivo studies have reported the osseointegration capability of Y-TZP zirconia implants quite similar to those on titanium implants since the surface modification techniques are well applied [7–11]. Grit-blasting has been commonly used to increase the titanium or zirconia roughness for adsorption of proteins, attachment of osteogenic cells, and bone formation [5, 8, 9, 22, 23]. Micro- and nano-scale surface modification influences the adsorption of extracellular matrix proteins, which regulate the adhesion of osteoblasts to the implant surface leading to cell proliferation and differentiation [5, 8, 24, 23]. However, the morphological aspects of zirconia surfaces cannot be controlled by using only ordinary surface modification such as grit-blasting since that provides a random texture on the surface.

Various methods of surface treatment have been proposed to improve the surface properties of zirconia implants [11, 22, 25–27]. Currently, surface modification on the implant surface via laser irradiation has gathering attention regarding the increase in roughness, wettability, and biological response without affecting the physical properties of zirconia [12, 14–16, 28, 23]. Morphological features (e.g., micro-grooves, pits, valleys, and peaks) on material surfaces can be controlled by using different intensity, type, time, and frequency of laser irradiation [12, 14, 28, 29].

Lasers can operate in either continuous mode (continuous wave—CW) or pulsed mode (PM), although the latter deliver the energy to the material in short (mili- to nano-seconds) or ultra-short (pico- to femto-seconds) periods of time (pulses). Various laser sources, working at different wavelengths and pulse duration have been studied aiming to modifying the surface of zirconia-based ceramics: Nd:YAG [30], Er:YAG [31],  $CO_2$  [32], Er, Cr:YSGG [33], and Nd:YVO<sub>4</sub> [34]. Considering zirconia is a brittle material it is highly sensitive to surface processing defects like pores and cracks, as the one produced for CW  $CO_2$  lasers or Nd:YAG lasers working short pulses (nanosecond regime) [35]. The presence of cracking is attributed to the (extensive) heat-affected zone generated by the thermal induced mechanisms developed by lasers working at the nanosecond regime and proved to be detrimental to the mechanical performance of zirconia [30, 35]. Alternatively, ultra-short pulsed lasers (pico- and femtosecond lasers) have been referred to produce ceramic-structured ceramic surfaces with minimal or no damages on the adjacent surfaces to the laser-machined ones [12, 13, 28]. The localized energy in very thin surface layers (< 100 nm) during very short times ( $10^{-15}$ – $10^{-12}$  s) can lead to surface ablation of material with negligible heat effects on the surrounding material, and thus

avoiding surface defects that are detrimental to the mechanical behavior of brittle materials.

The main aim of this study was to perform a literature review on the effects of laser irradiation of zirconia implants on their surface morphological aspects and biological response. It was hypothesized that laser irradiation is able to improve the surface morphologic features of zirconia implants leading to an enhanced biological response and osseointegration.

## Method

### Information sources and search strategy

An electronic search was performed on the PubMed database using the following search items: “zirconia” AND “laser” AND “surface modification” OR “surface treatment” AND “dental implants” OR “bone” OR “osteoblast” OR “osseointegration.” The inclusion criteria involved articles published in English language up to January 10, 2021 reporting studies on the modification of zirconia surfaces by laser irradiation. The eligibility inclusion criteria used for article searches also involved articles written in English, meta-analyses, randomized controlled trials, and prospective cohort studies. The exclusion criteria were the following: papers without abstract; case report with short follow-up period; studies focusing only on other surface modification methods. Also, a hand-search was performed on the reference lists of all primary sources and eligible studies of this systematic review for additional relevant publications. Studies based on publication date were not restricted during the search process. The present method was performed following the search strategy applied in previous integrative reviews 36–41.

### Study selection and data collection process

The articles retrieved from the search process were evaluated in three steps. The total of articles was compiled for each combination of key terms and therefore the duplicates were removed using Mendeley citation manager (Elsevier BV). Studies were primarily scanned for relevance by title, and the abstracts of those that were not excluded at this stage were assessed. The second step comprised the evaluation of the abstracts and non-excluded articles, according to the eligibility criteria on the abstract evaluation. Three of the authors (JCMS, BH, WFC) independently evaluated the titles and abstracts of potentially relevant articles.

A preliminary evaluation of the abstracts was carried out to establish whether the articles met the main aim of the study. Selected articles were individually read and evaluated concerning the purpose of this study. At last, the eligible articles received a study nomenclature label, combining first author

names and year of publication. Two reviewers independently organised the data, such as author names, journal, publication year, purpose, zirconia types, roughness, biological response, bone-to-implant contact (BIC) percentage, and laser parameters such as intensity, exposure time, laser type, wavelength, and application mode. Data of the reports were harvested directly into a specific data collection form to avoid multiple data recording regarding multiple reports within the same study (e.g., reports with different set-ups). Such evaluation was individually carried out by two researchers, followed by a joint discussion to ultimately select the relevant studies.

## Results

The bibliographic search on PubMed identified a total of 101 articles, as shown in Fig. 1. After excluding duplicates, 46 articles were evaluated by title and abstract although 31 were excluded because they did not meet the inclusion criteria. The remnant 15 articles were full read; although, 12 studies were considered relevant to the purpose of the present study taking into account a complete information on laser parameters, methods, and main outcomes.

Of the 12 selected articles, 7 studies were carried out in vitro while 5 studies were performed in vivo. The BIC percentage was evaluated by 4 studies while 3 studies evaluated the resorption of the bone crest. Laser surface treatment was morphologically characterized by in vitro articles although 4 studies evaluated the cellular response to the laser surface treatment. The main outcomes can be drawn as follow:

- The laser treatment of the surface promoted changes in the topography of the implant surface at the following levels of scale: mesoscale (e.g., grooves), micro-scale (e.g., peak/valley), nanoscale (e.g., nodules) [42]. The crystalline

structure of the zirconia can be maintained after laser treatment leading to the maintenance of the tetragonal phase [12, 14]. A nano-scale rough surface was noted in the micro-grooves of zirconia surfaces [14, 43–45].

- Different surface topographic aspects were associated with the different types of lasers used for surface modification: CW lasers (e.g., CO<sub>2</sub>) produced different levels of stochastic roughness while short or ultra-short pulsed lasers (e.g., nano, pico, or femtosecond lasers) were able to imprint different patterns to the surface.
- The laser surface treatment enhanced the adhesion, proliferation, and differentiation of osteoblasts on the zirconia surfaces, within 1 to 8 times of cell proliferation within the laser-treated groups compared to control groups [15, 16].
- In animal models, BIC percentage on laser-treated zirconia implants showed high mean values as found for zirconia surfaces with enhanced osseointegration [13, 46, 47]. When compared to the laser treatment produced on the surface of zirconia implants over grit-blasted and etched surfaces, the further laser treatment provided a higher degree of BIC [43]. However, laser-treated zirconia showed similar BIC values to the titanium surfaces treated by ordinary grit-blasting and etching procedures [13].
- Also, the laser-treated implants showed adequate levels of peri-implant bone crest maintenance ( $\sim 0.5 \pm 0.23$  mm) in the animal models over a period of 90 days.

## Discussion

### Zirconia implants

Zirconia has revealed remarkable clinical outcomes in the biomedical field, mainly in orthopedics and dentistry, due to the biological and mechanical response [6, 9, 21, 18, 19]. In the last years, zirconia has been used to develop teeth root canal posts, orthodontic brackets, implant abutments, and prosthetic infrastructures [48, 49, 19]. In the last 15 years, zirconia implants has increasingly become commercially available providing adequate esthetic, mechanical, and biological peri-implant outcomes [8, 20, 19, 23].

Zirconium dioxide (ZrO<sub>2</sub>) known as zirconia is a polymorphic ceramic, which has three distinct crystallographic phases: monoclinic (m), tetragonal (t), and cubic (c) [50] At room temperature, pure ZrO<sub>2</sub> has a monoclinic structure that remains stable up to 1170 °C [21]. It turns to the tetragonal zirconia when sintered at temperature between 1170 and 2370 °C while the cubic phase is reached between 2370 and 2680 °C [21, 18]. On cooling, the ZrO<sub>2</sub> tetragonal phase becomes monoclinic at a temperature around 970 °C [21]. The transformation pathway of tetragonal to the monoclinic

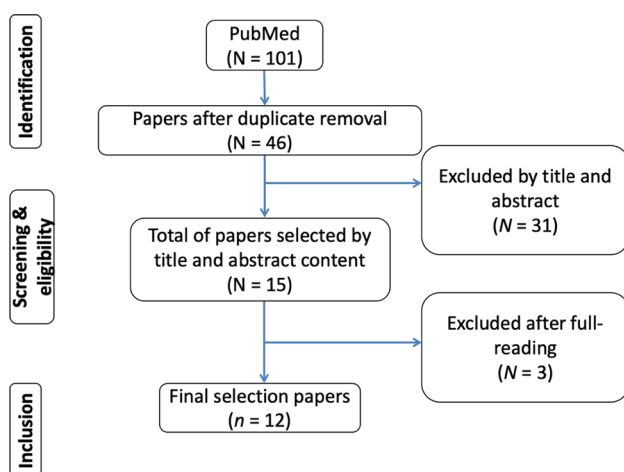
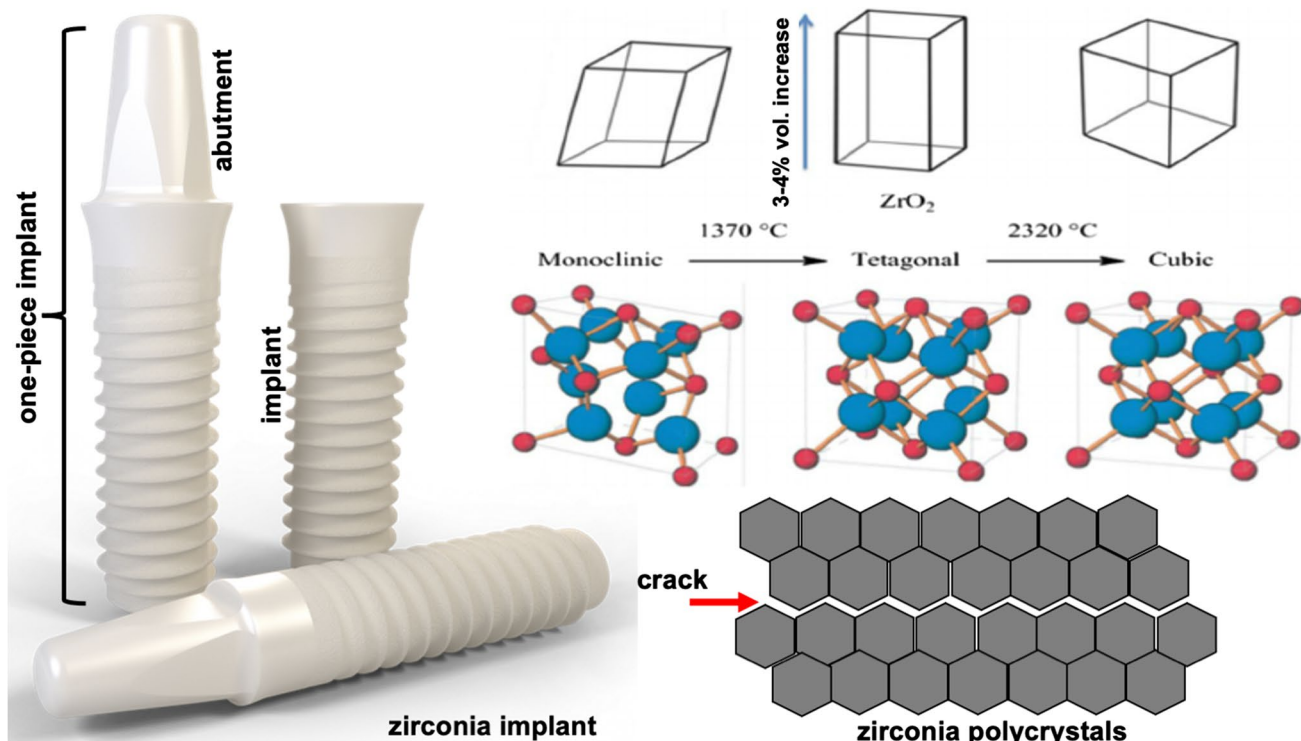


Fig. 1 Study selection flowchart

phase is associated with approximately 3 to 4% volumetric expansion that can lead to cracks [21, 50]. The mechanical properties of the zirconia are enhanced when the tetragonal phase is stabilized by adding small contents of oxides such as yttrium oxide (or yttria,  $Y_2O_3$ ), magnesium oxide (or magnesia, MgO), cerium oxide (or ceria,  $CeO_2$ ), and calcium oxide (or calcia, CaO) [21, 18]. For instance, yttria-stabilized zirconia polycrystals (YTZP) is produced by adding 2–5 mol% yttria to zirconia [21, 18]. That results in a significant increase in the flexural strength values at around 1200 MPa, elastic modulus at 230–270 GPa, and fracture toughness of approximately  $9\text{--}10\text{ MPa}\cdot\text{m}^{1/2}$  [20, 50]. On high stresses, oxide-stabilized zirconia has an inherent mechanism to inhibit the propagation of cracks. That consists in a transformation of the tetragonal to the monoclinic phase with an increase in the surrounding volume leading to the compression of the crack as seen in Fig. 2. However, YTZP is susceptible to degradation at low temperature when used in a humid environment as the one found in the oral cavity [20, 18, 51]. Tetragonal-to-monoclinic phase transformation can occur under fatigue conditions caused by cyclic stresses with origin in mastication loading and thermal oscillations. In this way, additive oxides such as alumina, ceria, or silica has been used to improve the resistance to low temperature degradation of zirconia [20, 21, 18, 51].

Topography, roughness, and chemical composition control the wettability and adsorption of proteins and ions (e.g.,  $Ca^{+2}$ ,  $PO^-$ ,  $OH^-$ ) onto the zirconia surface prior to the osseointegration [15, 16, 24, 25, 45]. Then, the activation of blood platelets and osteogenic cell migration follow the formation of the primary bioactive layer composed of ions and proteins [45, 23]. The differentiation of osteogenic cells and further formation of collagen matrix and bone tissue depend on the surface features and chemical interaction [45, 52, 23]. Several surface modifications have been proposed to enhance the surface behavior such as grit-blasting, calcium-based coatings, and laser-structuring protocols [10, 13, 17, 22–27]. Nevertheless, zirconia surface modification is a current challenge considering a balance among physical properties, chemical stability, and degradation behavior. Nowadays, most zirconia implants commercially available undergo surface treatment by grit-blasting, which produce non-homogeneous and random surface features under high risks of degradation [23]. Surface modification of zirconia by laser-structuring has been studied and therefore different procedures can be applied regarding the laser type, intensity, time, and mode [12–17, 28, 52]. In fact, the wettability and roughness of zirconia surfaces can be enhanced by laser-structuring while maintaining the degradation resistance, biocompatibility, and chemical interaction with the surrounding medium [14–16, 51, 45, 52].



**Fig. 2** Schematics of a zirconia implant (Straumann, Switzerland). Crystallographic phases of zirconia. Schematics of crack propagation which can occur among zirconia polycrystals prior to fracture

## Zirconia surface modification

Zirconia implants are often machined by using CAD-CAM systems that results in surfaces with micro-scale grooves or scratches leading to an average roughness ( $R_a$  parameter) at around 0.2–0.4  $\mu\text{m}$  [15, 42, 52, 23]. In a previous study, similar roughness values ( $\sim 0.3 \mu\text{m}$ ) were reported on machined MgO-PSZ [16, 45]. Wettability of the MgO-PSZ was measured by the contact angle of glycerol droplet of around  $79^\circ$  [16] while machined Y-PSZ revealed a mean value of  $82.4^\circ$  [15]. In another previous study, the average roughness of sintered Y-TZP was measured at around  $1.2 \pm 0.6 \mu\text{m}$  [17]. Sintered Y-TZP implants are produced with rough randomly surfaces once the micro-scale peak and valleys at the roughness profile depend on the zirconia powder particle size [12]. On the standard surfaces of Y-TZP implants modified by the grit-blasting method, the average roughness of machined Y-TZP can be increased due to the abrasive effect of airborne particles [14, 29]. As a consequence, morphological features such as micro-scale peaks and valleys are also randomly distributed over the grit-blasted and sintered zirconia surfaces. The average roughness of Y-TZP grit-blasted surfaces has been measured ranging from 1.2 up to 1.6  $\mu\text{m}$  [14, 29].

Nevertheless, morphological aspects of zirconia surfaces can be controlled by using the laser irradiation approach. Surfaces of different roughness have been produced by  $\text{CO}_2$  CW laser and patterned surfaces have been generated with short and ultra-short-pulsed lasers. Well-designed grooves, scratches, valleys, and peaks are produced at macro- and micro-scale width (1–100  $\mu\text{m}$ ) and micro-/submicron-scale depth (0.1–10  $\mu\text{m}$ ), as shown in Fig. 3 [42]. The roughness and wettability of laser-treated surfaces can also be adjusted considering the implant region and clinical considerations, as seen in Table 1 [14, 16, 45, 29]. In a previous study, a femtosecond laser irradiation (120 fs, 795 nm, 1 kHz)

was used to produce micro-scale pore patterns with 30  $\mu\text{m}$  diameter and 70  $\mu\text{m}$  pitch and micro-grooves with 30  $\mu\text{m}$  width and 70  $\mu\text{m}$  pitch on Y-TZP. The average roughness values of the micro-scale pores' patterns reached  $2.4 \pm 0.6 \mu\text{m}$  while micro-grooved surfaces showed roughness values of  $9.5 \pm 0.6 \mu\text{m}$ . That resulted in an effective surface contact area of 15% on micro-porous surfaces and 25% on micro-grooved surfaces [14, 29]. Another study reported the use of a femtosecond laser irradiation (800 nm, 1 kHz, 30mW) on A-Y-TZP surfaces leading to regular micro-scale grooves' patterns with 30  $\mu\text{m}$  width and 25  $\mu\text{m}$  depth [12]. Granular polycrystalline structures with dimensions of 1–6  $\mu\text{m}$  and nanostructures with sizes ranging from 30 to 100 nm were detected [14]. In fact, the modification at micro- and nano-scale increased the surface contact area for interaction with proteins and osteogenic cells.

Previous studies reported the modification of MgO-PSZ surfaces by using  $\text{CO}_2$  laser regarding different laser intensity [16, 45]. Morphologic aspects of the surfaces varied in function of the intensity such as crystal refurbishment on 0.6  $\text{kW}/\text{cm}^2$ ; hexagonal structure on 0.9  $\text{kW}/\text{cm}^2$ ; pores formation on 1.6  $\text{kW}/\text{cm}^2$ ; and dendrite on 2.5  $\text{kW}/\text{cm}^2$  [16, 45]. Consequently,  $R_a$  roughness increased as the power density of the laser irradiation increased (Table 1):  $R_a$  roughness was recorded at 0.3  $\mu\text{m}$  on 0.6  $\text{kW}/\text{cm}^2$ ; 0.33  $\mu\text{m}$  on 0.9  $\text{kW}/\text{cm}^2$ ; 0.71  $\mu\text{m}$  on 1.6  $\text{kW}/\text{cm}^2$ ; 1.8  $\mu\text{m}$  on 1.9  $\text{kW}/\text{cm}^2$ ; and 3.8  $\mu\text{m}$  on 2.5  $\text{kW}/\text{cm}^2$  [16, 45]. On the MgO-PSZ surfaces, the angle of contact of the glycerol droplet decreased as the roughness increased that indicates an increase in wettability:  $76^\circ$  on 0.6  $\text{kW}/\text{cm}^2$ ;  $62^\circ$  on 0.9  $\text{kW}/\text{cm}^2$ ;  $40^\circ$  on 1.6  $\text{kW}/\text{cm}^2$ ;  $50^\circ$  on 1.9  $\text{kW}/\text{cm}^2$ ; and  $54^\circ$  on 2.5  $\text{kW}/\text{cm}^2$  [16]. However, a significant decrease in the  $R_a$  roughness was detected on Y-PSZ when the  $\text{CO}_2$  laser intensity was increased; although, the morphological aspects also varied as a hexagonal microstructure appeared on 1.8  $\text{kW}/\text{cm}^2$ , while a porous microstructure was noted on 2.25  $\text{kW}/\text{cm}^2$ .

**Fig. 3** Illustration of surface morphological aspects produced by laser treatment on zirconia implants at different magnification scales: (A) macro-scale; (B,C) micro-scale; and (D,E) nano-scale texturization

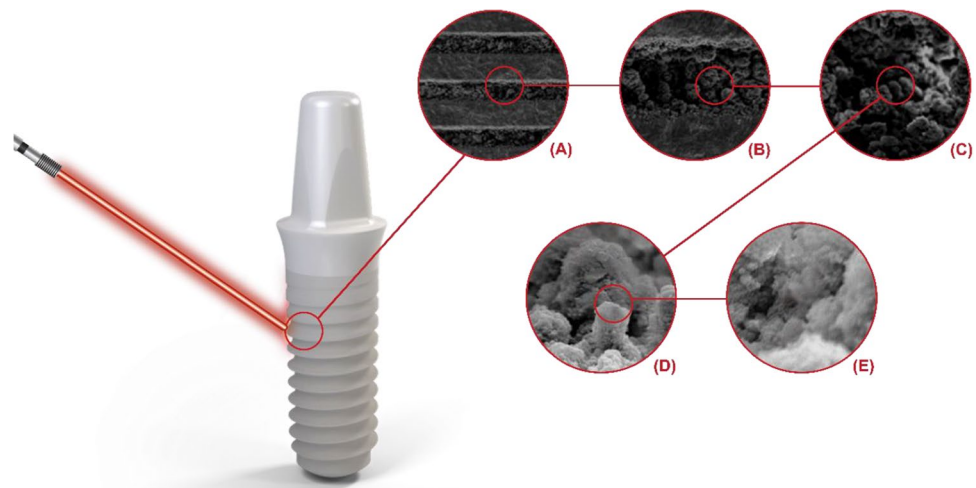


**Table 1** Relevant data extracted gathered from the selected studies

Authors (year)	Study design and follow-up	Implant specimens	Laser type	Laser parameters	Analyses of the materials	Main outcomes
Aivazi et al., (2016)	In vitro	A-3Y-TZP20 nano-composite discs, with an average grain size of $\leq 400$ nm	Femtosecond laser (Legend Elite Coherent Inc. company, USA) Wavelength of 800 nm	Laser pulses at 1000 Hz, 30mW at 0.50 mm/s	FESEM for surface inspection EDS for element analysis; XRD for chemical and phase composition analyses	The surface of the A-Y-TZP20 samples was modified to the micro-groove pattern. Reduction of contaminants incorporated in the previous stages of manufacture The material around the microstructures did not show phase transformation
Calvo-Guirado et al., (2013)	Animal study 6 male American Foxhound dogs aged 1 to 3 years and weighing between 18 and 20 kg. Each dog received 8 implants Follow-up: 1 or 3 months	48 implants, two groups: control–titanium implants test—zirconia Y-TZP implants White SKY® (Bredent Medical)	Femtosecond laser Tsunami™ Ti: Sapphire oscillator (Spectra Physics, Newport Corporation, Alberta, Canada) Wavelength of 795 nm	Laser pulses at 10nJ energy, with a repetition rate of 80 MHz	SEM for BIC EDX for Elemental analysis Histomorphometric analysis and measuring crestal bone height	After 1 month: BIC at 51.36% for Ti implants BIC at 44.68% for zirconia implants <i>Marginal bone resorption:</i> Zirconia implants at 0.01 mm Titanium implants at 0.77 mm After 3 months: BIC at 61.73% for Ti implants BIC at 47.94% for zirconia implants <i>Marginal bone resorption:</i> Zirconia for implants at 1.25 mm Titanium implants at 0.37 mm

Table 1 (continued)

Authors (year)	Study design and follow-up	Implant specimens	Laser type	Laser parameters	Analyses of the materials	Main outcomes
Calvo-Guirado et al., (2014)	Animal study 6 male American Foxhound dogs aged between 1 and 3 years and weighing from 18 to 20 kg. Each dog received 8 implants Follow-up: 30 or 90 days	48 zirconia implants (White Sky™) with 4 × 10 mm 24 with immediate loading; 24 without loading	Femtosecond laser	Femtosecond laser	SEM and optical microscopy for BIC; periosteal X ray for crestal bone height analysis	After 30 days BIC at 38.9% for immediately loaded and at 32% for non-loaded Crestal bone resorption at 0.58 ± 0.28 mm in the non-loaded group and at 0.5 ± 0.3 mm for immediately loaded group After 90 days BIC at 65% for immediately loaded group and at 57.6% for non-loaded Crestal bone resorption at 0.5 ± 0.23 mm in the immediately loaded group and at 0.56 ± 0.28 mm for non-loaded group
Calvo-Guirado et al., (2014)	Animal study 20 male New Zealand rabbits aged 30–35 weeks and weighing 3900–4500 g, placing two implants per tibia Follow-up: 1 or 4 weeks	80 implants, four groups: Group A) titanium implants, sandblasted and acid-etched Group B) zirconia implants and sandblasted Group C) titanium implants, sandblasted and acid-etched, supplemented with MLT 5% in solution Group D) zirconia implants, sandblasted and micro-grooved by femtosecond laser, supplemented with MLT 5% in solution	Femtosecond laser Tsunami™ Ti: Sapphire oscillator (Spectra Physics, Newport Corporation, Alberta, Canada) Wavelength of 795 nm	The system delivered 120 fs linearly polarized pulses with a repetition rate of 1 kHz. Pulse energy can reach a maximum of 1.1 mJ	SEM, optical microscopy for BIC EDX for elemental analysis	At 1 week: Group C (29.7 ± 2.4%) and group D (28.9 ± 1.3%) implants showed higher BIC % compared with group A and B After 4 weeks: group D showed the highest BIC% at 47.5 ± 2.2%

Table 1 (continued)

Authors (year)	Study design and follow-up	Implant specimens	Laser type	Laser parameters	Analyses of the materials	Main outcomes
DeIgado-Ruiz et al., (2011)	In vitro	66 cylindrical zirconia implants (3Y-TZP) 4 × 8 mm, three groups: Control group) without laser modification Group A) implants treated with femtosecond laser pulses to form pores Group B) implants treated with femtosecond laser pulses to form grooves	Femtosecond laser Tsunami™ Ti: Sapphire oscillator (Spectra Physics, Newport Corporation, Alberta, Canada) Wavelength of 795 nm	The system delivered 120 fs linearly polarized pulses with a repetition rate of 1 kHz	Optical interferometric profilometry for roughness analysis; SEM for surface characterization XRD for change in crystalline structure; EDX for elemental analysis	Ultra-fast laser ablation increased the roughness (Ra, Rq, Rz and Rt) significantly for the two texture patterns, from 1.2 × to 6 × times when compared to the control Significant decrease in contaminants were detected such as carbon (control 19.7% ± 0.8% > group B 8.4% ± 0.42% > group A 1.6% ± 0.35%) and aluminum (control 4.3% ± 0.9% > group B 2.3% ± 0.3% > group A 1.16% ± 0.2%) on laser-treated surfaces The tetragonal zirconia phase was preserved, while the traces of the monoclinic phase shown on the treated surfaces were reduced (control 4.32% > group A 1.94% > group B 1.72%)



Table 1 (continued)

Authors (year)	Study design and follow-up	Implant specimens	Laser type	Laser parameters	Analyses of the materials	Main outcomes
DeIgado-Ruiz et al., (2014)	Animal study 12 Foxhound dogs of approximately one year of age, each weighing between 14 to 15 kg, each mandible received 8 implants Follow-up: 1, 2 or 3 months	96 implants (4 mm × 10 mm), four groups: control group) Ti implants Group A) grit-blasted zirconia implants; Group B) zirconia implants treated with femtosecond laser pulses over 2 mm from the neck area; Group C) zirconia implants treated with femtosecond laser pulses over the entire endosseous surface	Femtosecond laser	Femtosecond laser	SEM for surface inspection EDX for elemental chemical composition analysis; Periotest for implant stability; X ray for crestal bone height analysis	Periotest values increased in all time points as a function of the extent of the microgrooves, as follows: group C > control > group B > group A ( $p < 0.05$ ) After 3 months: minimal bone loss for implants in groups C, B and control when compared to implants in group A ( $p < 0.05$ ). The implant surfaces of groups B and C showed extra bone growth inside the microgrooves that corresponded to the shape and direction of the microgrooves

Table 1 (continued)

Authors (year)	Study design and follow-up	Implant specimens	Laser type	Laser parameters	Analyses of the materials	Main outcomes
Hao et al., (2004)	In vitro Human osteoblast cell line (hFOB 1.19), (a) $1 \times 10^5$ cell/mL (cell fixation and morphology for 24 h), (b) $4 \times 10^5$ cells/mL (cell growth analysis for 7 days), (c) $1 \times 10^5$ cell/mL (cell count analysis for 14 days) Follow-up: 24 h and 7 or 14 days	Blocks ( $50 \times 12 \times 2.15$ mm) of zirconia partially stabilized with 4% magnesia (MgO-PSZ)	CO <sub>2</sub> laser (3 kW) Wavelength of 10.6 $\mu$ m	Laser used at 0.6, 0.9, 1.6, 1.9, or 2.5 kW/cm <sup>2</sup> , 10.6 $\mu$ m wavelength, travel speed was adjusted to 2000 mm/min	SEM for cell morphology, cell adhesion and zirconia surface; sessile drop measuring machine (First Ten Angstroms, Inc) for wettability; profilometer for zirconia roughness analysis; XRD for chemical phase and crystalline inspection	Cell growth, compared with the untreated one: 0.6 kW/cm <sup>2</sup> increase of 17%; 0.9 kW/cm <sup>2</sup> double cover density; 1.6 kW/cm <sup>2</sup> triple cover density; 1.9 kW/cm <sup>2</sup> triple cover density; The cell coverage area did not increase further at higher power density of 2.5 Roughness (Ra): 0.295 $\mu$ m for untreated 0.305 $\mu$ m for 0.6 kW/cm <sup>2</sup> 0.333 $\mu$ m for 0.9 kW/cm <sup>2</sup> 0.717 $\mu$ m for 1.6 kW/cm <sup>2</sup> 1.882 $\mu$ m for 1.9 kW/cm <sup>2</sup> 3.854 $\mu$ m for 2.5 kW/cm <sup>2</sup> Wettability: glycerol sessile drop 79° for untreated 76° for 0.6 kW/cm <sup>2</sup> 62° for 0.9 kW/cm <sup>2</sup> 40° for 1.6 kW/cm <sup>2</sup> 50° for 1.9 kW/cm <sup>2</sup> 54° for 2.5 kW/cm <sup>2</sup>

Table 1 (continued)

Authors (year)	Study design and follow-up	Implant specimens	Laser type	Laser parameters	Analyses of the materials	Main outcomes
Hao et al., (2004)	In vitro Acellular human SBF (ion concentration almost equal to that of human blood plasma) Follow-up: 14 days	Blocks (50 × 12 × 2.15 mm) of zirconia partially stabilized with 4% magnesia (MgO-PSZ)	CO <sub>2</sub> laser wavelength of 10.6 μm	3 kW, used at: 0.6 kW/cm <sup>2</sup> , 0.9 kW/cm <sup>2</sup> , 1.6 kW/cm <sup>2</sup> , 1.9 kW/cm <sup>2</sup> , 2.5 kW/cm <sup>2</sup> , 10.6 μm wavelength, travel speed was adjusted to 2000 mm/min	Wettability on sessile drop measuring machine (First Ten Angstroms, Inc); Profilometer for roughness analysis; SEM, OM, XRD-microstructure and crystal size	The Ra roughness increased as the laser power density increased. The roughness (Ra) was recorded at: 0.295 μm (untreated), 0.305 μm (0.6 kW/cm <sup>2</sup> ), 0.333 μm (0.9 kW/cm <sup>2</sup> ), 0.717 μm (1.6 kW/cm <sup>2</sup> ), 1.882 μm (1.9 kW/cm <sup>2</sup> ), 3.854 μm (2.5 kW/cm <sup>2</sup> ) The shape of the surface microstructure varied with the different power density of the CO <sub>2</sub> laser applied: crystal rearrangement (0.6 kW/cm <sup>2</sup> ), hexagonal structure (0.9 kW/cm <sup>2</sup> ), cell formation (1.6 kW/cm <sup>2</sup> ) uniform cell formation (1.9 kW/cm <sup>2</sup> ), and coral and dendritic (2.5 kW/cm <sup>2</sup> ) Improve the bioactivity of the MgO-PSZ surface, generating a functional group to facilitate the formation of bone apatite's

Table 1 (continued)

Authors (year)	Study design and follow-up	Implant specimens	Laser type	Laser parameters	Analyses of the materials	Main outcomes
Hao et al., (2005)	In vitro Human osteoblast cell line (hFOB 1.19), at $4 \times 10^5$ cells/mL Follow-up: 1 week	5% yttria partially stabilized zirconia (Y-PSZ)	CO <sub>2</sub> laser Wavelength of 10.6 $\mu$ m	CO <sub>2</sub> laser: 3 kW, used at 1.80 kW/cm <sup>2</sup> , 2.25 kW/cm <sup>2</sup> 10.6 $\mu$ m wavelength, travel speed was adjusted to 5000 mm/min	Wettability on sessile drop measuring machine (First Ten Angstroms, Inc); SEM—cell culture and adhesion	In the treated samples, there was a decrease in roughness and a solidified microstructure. Increased wettability characteristics and better adhesion of osteoblastic cells Wettability: glycerol 82.4° (untreated), 74.2° (1.80 kW/cm <sup>2</sup> ), 70.5° (2.25 kW/cm <sup>2</sup> ) The shape of the surface microstructure varied with the different power densities of the CO <sub>2</sub> laser applied: hexagonal structure (1.8 kW/cm <sup>2</sup> ), cell microstructure (2.25 kW/cm <sup>2</sup> )
Hirota et al., (2019)	Animal study 12 male Wistar rats, each weighing approximately 180 g and 6 weeks old. Each animal received an implant, in the femur Follow-up: 4 weeks	12 implants (rectangular plates 3 × 2 × 1 mm) a) laser/3Y-TZP; b) G2- laser/A-10Ce-TZP30; c) G3 – blasted HF/3Y-TZP; d) G4-blasted HF/A-10Ce-TZP30	Nd:YAG nanosecond-pulsed; wavelength of 1064 nm	Laser pulsed at 3 ns; 150 $\mu$ J/pulse; 50 Hz; 7 $\mu$ m/s	SEM for surface characterization; EDX for elemental analysis; CLSM for BIC and bone formation	Production of nanoscale surface topography inside the micro-grooves of Y-TZP and Ce-TZP Laser treatment was effective to increase BIC for Y-TZP (78.9 ± 6.57%), but not for Ce-TZP (14.0 ± 2.43%). BIC of laser implants/Y-TZP was significantly the highest among the four different implants (p < 0.05) Surface chemistry influenced bone formation separately from surface morphology

Table 1 (continued)

Authors (year)	Study design and follow-up	Implant specimens	Laser type	Laser parameters	Analyses of the materials	Main outcomes
Nassif et al., (2018)	In vitro Saos-2 (primary human osteosarcoma) cells at $50 \times 10^3$ /mL Follow-up: 3 days or 1 week	80 zirconia disks ( $19.5 \times 3$ mm): ZrO <sub>2</sub> + HfO <sub>2</sub> + Y <sub>2</sub> O <sub>3</sub> ; > 99.0 Y <sub>2</sub> O <sub>3</sub> ; 4.5–5.6 HfO <sub>2</sub> ; < 5Al <sub>2</sub> O <sub>3</sub> ; < 0.5; other oxides: < 0.5) Four groups: a) sintered (AS—control); b) Group II: Rocatec (ROC); c) Group III: laser (LAS) d) Group IV: SIE	Er, Cr: YSGG laser (BIOL/ASE, California, USA) Wavelength of 2780 nm	Frequency at 20 Hz; power at 3 W	Vickers microhardness; AFM for surface morphology and topography; SEM for microstructural hemocytometer for cell number and density	Cell count: 3 days—SIE ( $53.5 \pm 2.2$ ) > AS ( $51 \pm 1.4$ ) > LAS ( $23 \pm 1.9$ ) > ROC ( $21.5 \pm 1$ ) 7 days—SIE ( $108 \pm 1.7$ ) > AS ( $72 \pm 2.1$ ) > LAS ( $37.5 \pm 1.2$ ) > ROC ( $32 \pm 1.4$ ) Roughness (Ra): ROC ( $2.201 \pm 0.352 \mu\text{m}$ ) > LAS ( $1.412 \pm 0.166 \mu\text{m}$ ) > SIE ( $0.830 \pm 0.098 \mu\text{m}$ ) > AS ( $0.475 \pm 0.027 \mu\text{m}$ )
Soares et al., (2016)	In vitro MC3T3-E1 osteoblast cells, line derived from mouse tissue, $1 \times 10^4$ cells/mL Follow-up: 3 or 7 days	48 Y-TZP blocks (92% ZrO <sub>2</sub> , 5% Y <sub>2</sub> O <sub>3</sub> , HfO <sub>2</sub> < 3%, Al <sub>2</sub> O <sub>3</sub> , SiO <sub>2</sub> < 1%) were divided into 4 groups: a) (no laser irradiation); b) (1.5 W); c) (3.0 W); d) (5.0 W)	Er,Cr: YSGG laser (Waterlase, Biolase Technology Inc, Irvine, CA) Wavelength of 2,780 nm	Laser used at: 1.5 W; 3.0 W; 5.0 W; 30 s; 20 Hz	Confocal xwhite light microscope for roughness and topography; SEM for zirconia surface morphology, cellular morphology; MTT for cell adhesion and proliferation	Roughness (Ra): a) $1.26 \pm 0.6$ , b) $1.52 \pm 2.0$ , c) $1.14 \pm 0.7$ , d) $0.70 \pm 0.3$ After 3 days, cell response higher than the control group: a) 1.4%, b) 3.1% c) 4.5% After 7 days, there was no difference between groups

The mean values of the contact angle of the glycerol droplet also decreased with the increase in laser power: 74.2° was recorded on 1.80 kW/cm<sup>2</sup>, while an angle of 70.5° was recorded on 2.25 kW/cm<sup>2</sup> [15].

On Er, Cr: YSGG laser at low level irradiation, no significant changes were detected on Y-TZP using the following parameters: 1.5 W (*Ra* of 1.52 ± 2.0 μm and *Sa* of 1.78 ± 2.0 μm); 3.0 W (*Ra* of 1.14 ± 0.7 μm and *Sa* of 1.24 ± 1.3 μm); and 5.0 W (*Ra* of 0.70 ± 0.3 μm and *Sa* of 1.36 ± 1.0 μm) [17]. However, micro-scale scratches and grooves were detected in another study assessing a laser irradiation of 3 W on Y-TZP surface that resulted in a *Ra* roughness at 1.41 ± 0.166 μm and *Rz* roughness at 5.1 ± 0.327 μm [44]. A fiber laser was also used to produce changes on the Y-TZP surfaces, and therefore the results revealed regular edges' pattern leading to an increase in roughness at around 10 times (*Sa* of 1.75 ± 0.32 μm) when compared to machined surfaces (*Sa* of 0.18 ± 0.04 μm) [52].

### Biological response to surface characteristics produced by laser

In vitro studies on cell culture have shown stimuli of the osteogenic cell response on laser-treated zirconia, as illustrated in Table 1 [15–17]. For instance, zirconia surface treated with CO<sub>2</sub> laser revealed a significant increase in the osteogenic cell proliferation by 70–90% when compared to untreated zirconia [15, 16]. The laser energy used in the surface treatment of zirconia has an active effect on the surface morphologic aspects, which in turn influenced the osteogenic cell behavior [15–17]. The osteogenic cell proliferation is significantly increased when the laser intensity was increased [15–17]. A progressive increase in cell proliferation was noted on Y-TZP irradiated with Er, Cr: YSGG laser with wavelength of 2780 nm, for 30 s and 20 Hz on 1.5 W, 3 W, or 5 W when compared to untreated zirconia [17]. Another study with Er, Cr: YSGG laser at 20 Hz and 3 W reported a significant difference in cell proliferation for 3 and 7 days cell incubation. Viable cell count was measured at  $[23 \pm 1.9] \times 10^3$  and  $[37.5 \pm 1.2] \times 10^3$  for laser-treated Y-TZP and  $[51 \pm 1.4] \times 10^3$  and  $[72 \pm 2.1] \times 10^3$  for untreated zirconia [44].

The morphological aspects of the osteoblast have been reported in previous studies by evaluating projections of cytoplasm, namely phyllopodia, and the spreading of the cell over the surfaces [15–17, 42, 52]. The cells exhibited a final stage of cell adhesion, showing more flattened and with a higher cytoplasmic projection with phyllopod that extended about 50–60 μm beyond the cells when compared to smaller phyllopods (5 to 10 μm projections) on untreated surfaces [15, 16]. The degree of maturation achieved by osteoblasts after contact with laser-treated Y-TZP surfaces is another important aspect to be considered, since it is a key factor

for the production of the bone matrix [42, 52]. A higher degree of cell differentiation on laser-treated surfaces was validated by measuring osteogenic genes, such as collagen type I, osteopontin, osteocalcin, and BMP-2 [42]. Results showed values ranging from 7 up to 25 times higher for laser-treated Y-TZP compared to untreated surfaces over a period of 7-days incubation [42]. Remarkable changes in cell morphologic aspects were evaluated by a previous study [52] at approximately 3 times for irradiated Y-TZP when compared to the non-irradiated Y-TZP [52]. The morphologic changes were linked to an increase in the gene expression of Runx2 mRNA, alkaline phosphatase, and oxytocin mRNA for 3, 7, and 14 days incubation, respectively [52]. Those are essential transcriptional factors for the differentiation of osteoblasts. Thus, laser-assisted surface modifications increased the gene expression related to time-dependent osteogenic differentiation.

Studies have shown similar BIC values for titanium or zirconia implant surfaces treated with laser irradiation [13, 46, 53]. In American Foxhound dogs, mean BIC percentage was recorded at 44.6 ± 17.6% on zirconia for 1 month and 47.9 ± 16% for 3 months. No statistically differences were found when compared to titanium implant surfaces regarding the BIC mean values at 51.3 ± 12% for 1 month and at 61.7 ± 16.2% for 3 months [13]. In another study in American Foxhound dogs, laser-treated zirconia implant surfaces showed the BIC mean values at 22.8 ± 1.5% for 1 week and 37.5 ± 2.1% for 4 weeks [46]. Those values were also not statistically different when compared to BIC values for titanium surfaces: 25.4 ± 1.2% for 1 week and 38.4 ± 1.8% for 4 weeks [46]. Similar results were found in another study in New Zealand white rabbits regarding the BIC mean values recorded on laser-treated zirconia implants at 39.97 ± 13.19% for 6 weeks and 43.87 ± 14.54% for 12 weeks in comparison to BIC mean values on titanium implant surfaces at 34.15 ± 10.34% for 6 weeks and 34.82 ± 12.21% for 12 weeks [53]. Thus, the laser treatment is capable of modifying the surface topographic aspects of zirconia for an enhanced osseointegration as compared to titanium implant surfaces [14, 46]. BIC studies in Wistar rats showed no statistically differences between Y-TZP (56.2 ± 3.56%) and Ce-TZP (37.1 ± 14.01%) with grit-blasted surface treatment and acidic etching for 4 weeks [43]. However, the laser-treated Y-TZP surfaces by using Nd:YAG wavelength 1064 nm, pulse of 3 ns, 50 Hz, and 150 mJ/pulse revealed higher BIC mean values (78.9 ± 6.57%) when compared to laser-treated Ce-TZP (14.0 ± 2.43%) [43].

In the comparison between machined and laser-treated Y-TZP implants, within a period of 4 weeks, BIC mean values were 2 times higher (81.9 ± 20.4%) in the cortical bone portion in the Sprague–Dawley rats when compared to those for machined Y-TZP surfaces (39.8 ± 19.2%).

In the cancellous bone portion, BIC mean values did not show significant differences [52]. In the evaluation of the BIC percentage between zirconia implants with different surface treatments, no statistically significant differences were found between the Y-TZP surfaces with different surface treatments for 6 or 12 weeks respectively:  $33 \pm 14\%$  and  $33.7 \pm 14.5\%$  on sintered zirconia;  $39.6 \pm 15\%$  and  $41.3 \pm 15.8\%$  on grit-blasted; and  $39.97 \pm 13.19\%$  and  $43.87 \pm 14.54\%$  on laser-treated surface [53]. Regarding occlusal loading, Y-TZP implants treated with femtosecond lasers, subjected to immediate loading, showed higher BIC values for 1 month ( $38.9 \pm 6.68\%$ ) and 3 months ( $65 \pm 4.36\%$ ) when compared to the same implant condition free of occlusal loading ( $32 \pm 3.65\%$ ) for 1 month and ( $57.6 \pm 3.62\%$ ) for 3 months. Findings revealed a statistically significant improvement of the BIC percentage when implants were immediately loaded [47].

In a Foxhound dogs model, Y-TZP zirconia implants treated with femtosecond laser (100 fs, 795 nm, 10 nJ, 80 MHz), near-infrared wavelengths 795 nm and 10 nJ energy with a 80 MHz, showed marginal bone crest resorption values at  $0.01 \pm 0.57$  mm for 1 month and at  $1.25 \pm 1.73$  mm for 3 months [13]. These values were statistically significant only in the 3-month period when compared to the marginal bone crest resorption values in titanium implants:  $0.77 \pm 0.69$  mm for 1 month and  $0.37 \pm 0.34$  mm for 3 months [13]. Another study reported findings on Y-TZP zirconia implants treated by using femtosecond on the entire implant body or only on the implant neck [29]. After 3 months, zirconia implants treated with laser at the neck region revealed a higher crestal bone loss ( $0.36 \pm 0.01$  mm) when compared to the implants treated in the entire contact surfaces ( $0.26 \pm 0.01$  mm) [46]. Immediately, loaded Y-TZP zirconia implants showed crestal bone loss values of  $0.5 \pm 0.3$  mm for 1 month and  $0.5 \pm 0.23$  mm for 3 months [47].

## Conclusions

Within the limitations of the previous studies, the following outcomes can be drawn:

- The surface treatment performed by laser-assisted techniques generated changes in the surface roughness parameters, producing textures at meso-, micro-, and nano-scale leading to an enhanced surface wettability.
- The laser treatment produced a favorable response in the initial levels of adhesion and proliferation of osteoblasts on the zirconia surface when compared to untreated zirconia surfaces.
- A high BIC percentage was recorded on the laser-treated zirconia surfaces that corresponded to enhanced

osseointegration. Similar values of bone-implant contact were found on standard titanium implants and laser-treated zirconia implants.

- Further studies are required to establish optimum processing parameters for each type of laser used in the surface treatment of different zirconia-based materials.

**Funding** The authors acknowledge the support provided by the following FCT-Portugal projects: UID/EEA/04436/2013, SFRH/BPD/123769/2016, and LaserMULTICER [POCI-01-0145-FEDER-031035].

## Declarations

**Conflict of interests** The authors declare no conflict of interests.

## References

1. Adell R, Hansson BO, Brånemark PI, Breine U (1970) Intraosseous anchorage of dental prostheses. *Scand J Plast Reconstr Surg Hand Surg* 4:19–34. <https://doi.org/10.3109/02844317009038440>
2. Brånemark PI, Adell R, Albrektsson T, Lekholm U, Lundkvist S, Rockler B (1983) Osseointegrated titanium fixtures in the treatment of edentulousness. *Biomaterials* 4:25–28. [https://doi.org/10.1016/0142-9612\(83\)90065-0](https://doi.org/10.1016/0142-9612(83)90065-0)
3. Souza JCM, Sordi MB, Kanazawa M, Ravindran S, Henriques B, Silva FS, Aparicio C, Cooper LF (2019) Nano-scale modification of titanium implant surfaces to enhance osseointegration. *Acta Biomater.* 94:112–131. <https://doi.org/10.1016/j.actbio.2019.05.045.E>
4. Brånemark R, Öhrnell LO, Nilsson P, Thomsen P, Tool T, Suwandi JS, Toes REM, Nikolic T, Roep BO, Ferguson SJ et al (2008) Biomechanical characterization of osseointegration during healing: an experimental in vivo study in the rat. *Clin Exp Rheumatol* 18:97–103. <https://doi.org/10.1002/jbm.a>
5. Bergemann C, Duske K, Nebe JB, Schöne A, Bulnheim U, Seitz H, Fischer J (2015) Microstructured zirconia surfaces modulate osteogenic marker genes in human primary osteoblasts. *J Mater Sci Mater Med* 26:1–11. <https://doi.org/10.1007/s10856-014-5350-x>
6. Albrektsson T, Sennerby L, Wennerberg A (2000) State of the art of oral implants. *Periodontol* 2008(47):15–26. <https://doi.org/10.1111/j.1600-0757.2007.00247.x>
7. Gahlert M, Roehling S, Sprecher CM, Kniha H, Milz S, Bormann K (2011) In vivo performance of zirconia and titanium implants: a histomorphometric study in mini pig maxillae. *Clin Oral Implants Res* 23:281–286. <https://doi.org/10.1111/j.1600-0501.2011.02157.x>
8. Depprich R, Zipprich H, Ommerborn M, Naujoks C, Wiesmann H-P, Kiattavorncharoen S, Lauer H-C, Meyer U, Kübler NR, Handschel J (2008) Osseointegration of zirconia implants compared with titanium: an in vivo study. *Head Face Med* 4:30. <https://doi.org/10.1186/1746-160X-4-30>
9. Depprich R, Ommerborn M, Zipprich H, Naujoks C, Handschel J, Wiesmann HP, Kübler NR, Meyer U (2008) Behavior of osteoblastic cells cultured on titanium and structured zirconia surfaces. *Head Face Med* 29:1–9. <https://doi.org/10.1186/1746-160X-4-29>

10. Rocchietta I, Fontana F, Addis A, Schupbach P, Simion M (2009) Surface-modified zirconia implants: tissue response in rabbits. *Clin Oral Implants Res* 20:844–850. <https://doi.org/10.1111/j.1600-0501.2009.01727.x>
11. Schliephake H, Hefti T, Schlottig F, Gédet P, Staedt H (2010) Mechanical anchorage and peri-implant bone formation of surface-modified zirconia in minipigs. *J Clin Periodontol* 37:818–828. <https://doi.org/10.1111/j.1600-051X.2010.01549.x>
12. Aivazi M, hossein Fathi M, Nejatidanesh F, Mortazavi V, HashemiBeni B, Matinlinna JP, Savabi O (2016) The evaluation of prepared microgroove pattern by femtosecond laser on alumina-zirconia nano-composite for endosseous dental implant application. *Lasers Med Sci* 31:1837–1843. <https://doi.org/10.1007/s10103-016-2059-8>
13. Calvo-Guirado JL, Aguilar-Salvatierra A, Delgado-Ruiz RA, Negri B, Fernández MPR, Maté Sánchez de Val JE, Gómez-Moreno G, Romanos GE (2013) Histological and histomorphometric evaluation of zirconia dental implants modified by femtosecond laser versus titanium implants: an experimental study in fox hound dogs. *Clin Implant Dent Relat Res* 17:525–532. <https://doi.org/10.1111/cid.12162>
14. Delgado-Ruiz RA, Calvo-Guirado JL, Moreno P, Guardia J, Gomez-Moreno G, Mate-Sánchez JE, Ramirez-Fernández P, Chiva F (2011) Femtosecond laser microstructuring of zirconia dental implants. *J Biomed Mater Res Part B Appl Biomater*. 96 B:91–100. <https://doi.org/10.1002/jbm.b.31743>
15. Hao L, Lawrence J, Chian KS (2005) Osteoblast cell adhesion on a laser modified zirconia based bioceramic. *J Mater Sci Mater Med* 16:719–726. <https://doi.org/10.1007/s10856-005-2608-3>
16. Hao L, Lawrence J, Chian KS (2004) Effects of CO<sub>2</sub> laser irradiation on the surface properties of magnesia-partially stabilised zirconia (MgO-PSZ) bioceramic and the subsequent improvements in human osteoblast cell adhesion. *J Biomater Appl* 19:81–105. <https://doi.org/10.1177/0885328204043546>
17. Soares RD, Rodrigues JA, Cassoni A, Cruz A, Simoes CO, Pasqua-Neto JD, Gehrke SA, Blay A, Cesar PF, Shibli JA (2016) In vitro behavior of osteoblasts on zirconia after different intensities of erbium, chromium-doped: yttrium, scandium, gallium, and garnet-laser irradiation. *J Craniofac Surg* 27:784–788. <https://doi.org/10.1097/SCS.0000000000002429>
18. Zhang Y, Lawn BR (2018) Novel Zirconia Materials in Dentistry. *J Dent Res* 97(2):140–147. <https://doi.org/10.1177/0022034517737483>
19. Pessanha-Andrade M, Sordi MB, Henriques B, Silva FS, Teughels W, Souza JCM (2018) Custom-made root-analogue zirconia implants: A scoping review on mechanical and biological benefits. *J Biomed Mater Res B Appl Biomater*. 106(8):2888–2900. <https://doi.org/10.1002/jbm.b.34147>
20. Zhang Y (2012) Overview: Damage resistance of graded ceramic restorative materials. *J Eur Ceram Soc* 32(11):2623–2632. <https://doi.org/10.1016/j.jeurceramsoc.2012.02.020>
21. Garvie RC, Hannink RH, Pascoe RT (1975) Ceramic steel? *Nature* 258:703–704. <https://doi.org/10.1038/258703a0>
22. Gahlert M, Gudehus T, Eichhorn S, Steinhäuser E, Kniha H, Erhardt W (2007) Biomechanical and histomorphometric comparison between zirconia implants with varying surface textures and a titanium implant in the maxilla of miniature pigs. *Clin Oral Implants Res* 18:662–668
23. Schünemann FH, Galárraga-Vinueza ME, Magini R, Fredel M, Silva F, Souza JCM, Zhang Y, Henriques B (2019) Zirconia surface modifications for implant dentistry. *Mater Sci Eng C Mater Biol Appl*. 98:1294–1305. <https://doi.org/10.1016/j.msec.2019.01.062>
24. Gouveia PF, Mesquita-Guimarães J, Galárraga-Vinueza ME, Souza J, Silva FS, Fredel MC, Boccaccini AR, Detsch R, Henriques B (2021) In-vitro mechanical and biological evaluation of novel zirconia reinforced bioglass scaffolds for bone repair. *J Mech Behav Biomed Mater* 114:104164. <https://doi.org/10.1016/j.jmbbm.2020.104164>
25. Peñarrieta-Juanito G, Cruz M, Costa M, Miranda G, Marques J, Magini R, Mata A, Souza JCM, Caramês J, Silva FS (2018) A novel gradated zirconia implant material embedding bioactive ceramics: Osteoblast behavior and physicochemical assessment. *Materialia* 1:3–14. <https://doi.org/10.1016/j.mtla.2018.07.002>
26. Hirota M, Hayakawa T, Ohkubo C, Sato M, Hara H, Toyama T, Tanaka Y (2014) Bone responses to zirconia implants with a thin carbonate-containing hydroxyapatite coating using a molecular precursor method. *J Biomed Mater Res Part B Appl Biomater*. 102:1277–1288. <https://doi.org/10.1002/jbm.b.33112>
27. Lee J, Sieweke JH, Rodriguez NA, Schüpbach P, Lindström H, Susin C, Wikesjö UME (2009) Evaluation of nano-technology-modified zirconia oral implants: a study in rabbits. *J Clin Periodontol* 36:610–617. <https://doi.org/10.1111/j.1600-051X.2009.01423.x>
28. Han J, Zhang F, Van Meerbeek B, Vleugels J, Braem A, Castagne S (2021) Laser surface texturing of zirconia-based ceramics for dental applications: A review. *Mater Sci Eng C Mater Biol Appl* 123:112034. <https://doi.org/10.1016/j.msec.2021.112034>
29. Delgado-Ruiz RA, Marković A, Calvo-Guirado JL, Lazić Z, Piatelli A, Boticelli D, Maté-Sánchez JE, Negri B, Ramírez-Fernández MP, Mišić T (2014) Implant stability and marginal bone level of microgrooved zirconia dental implants: a 3-month experimental study on dogs. *Vojnosanit Pregl* 71:451–461. <https://doi.org/10.2298/VSP121003034D>
30. Henriques B, Hammes N, Souza JCM, Özcan M, Mesquita-Guimarães J, Silva FS, Fredel MC, Volpato CM, Carvalho O (2020) Influence of ns-Nd:YAG laser surface treatment on the tensile bond strength of zirconia to resin-matrix cements. *Ceramics International* 46(17):27822–27831. <https://doi.org/10.1016/j.ceramint.2020.07.281>
31. Gomes AL, Ramos JC, Santos-del Riego S, Montero J, Albaladejo A (2015) Thermocycling effect on microshear bond strength to zirconia ceramic using Er:YAG and tribochemical silica coating as surface conditioning. *Lasers Med Sci*. <https://doi.org/10.1007/s10103-013-1433-z>
32. Paranhos MPG, Burnett LH, Magne P (2011) Effect Of Nd:YAG laser and CO<sub>2</sub> laser treatment on the resin bond strength to zirconia ceramic. *Quintessence Int*
33. Aras WMF, Barroso JSM, Blay A, Rodrigues JA, Cassoni A (2016) Er, Cr:YSGG laser irradiation influence on Y-TZP bond strength to resin cement. *Ceram Int*. <https://doi.org/10.1016/j.ceramint.2016.05.180>
34. Abu Ruja M, De Souza GM, Finer Y (2019) Ultrashort-pulse laser as a surface treatment for bonding between zirconia and resin cement. *Dent Mater*. <https://doi.org/10.1016/j.dental.2019.07.009>
35. Rocca J-P, Fornaini C, Brulat-Bouchard N, Bassel Seif S, Darque-Ceretti E (2014) CO<sub>2</sub> and Nd:YAP laser interaction with lithium disilicate and Zirconia dental ceramics: a preliminary study. *Opt Laser Technol* 57:216–223. <https://doi.org/10.1016/j.optlastec.2013.10.008>
36. Souza JCM, Fernandes V, Correia A, Miller P, Carvalho O, Silva FS, Özcan M, Henriques B, Surface modification of glass fiber-reinforced composite posts to enhance their bond strength to resin-matrix cements: an integrative review. *Clinical Oral Investigations* <https://doi.org/10.1007/s00784-021-04221-y>
37. Lopes-Rocha L, Ribeiro-Gonçalves L, Henriques B, Özcan M, Tiritan ME, Souza JCM (2021) An integrative review on the toxicity of Bisphenol A (BPA) released from resin composites used in dentistry. *Journal of Biomedical Materials Research Part B: Applied Biomaterials* 109(11):1942–1952. <https://doi.org/10.1002/jbm.b.34843>



38. Fernandes V, Silva AS, Carvalho O, Henriques B, Silva FS, Özcan M, Souza JCM (2021) The resin-matrix cement layer thickness resultant from the intracanal fitting of teeth root canal posts: an integrative review. *Clinical Oral Investigations* 25(10):5595–5612. <https://doi.org/10.1007/s00784-021-04070-9>
39. Tafur-Zelada C, Carvalho O, Silva FS, Henriques B, Özcan M, Souza JCM (2021) The influence of zirconia veneer thickness on the degree of conversion of resin-matrix cements: an integrative review. *Clinical Oral Investigations* 25(6):3395–3408. <https://doi.org/10.1007/s00784-021-03904-w>
40. Messous R, Henriques B, Bousbaa H, Silva FS, Teughels W, Souza JCM (2021) Cytotoxic effects of submicron- and nano-scale titanium debris released from dental implants: an integrative review. *Clinical Oral Investigations* 25(4):1627–1640. <https://doi.org/10.1007/s00784-021-03785-z>
41. Souza JCM, Pinho SS, Pranto Braz M, Silva FS, Henriques B (2021) Carbon fiber-reinforced PEEK in implant dentistry: A scoping review on the finite element method. *Computer Methods in Biomechanics and Biomedical Engineering* 24(12):1355–1367. <https://doi.org/10.1080/10255842.2021.1888939>
42. Rezaei NM, Hasegawa M, Ishijima M, Nakhaei K, Okubo T, Taniyama T, Ghassemi A, Tahsili T, Park W, Hirota M et al (2018) Biological and osseointegration capabilities of hierarchically (meso-/micro-/nano-scale) roughened zirconia. *Int J Nanomedicine* 13:3381–3395. <https://doi.org/10.2147/IJN.S159955>
43. Hirota M, Harai T, Ishibashi S, Mizutani M, Hayakawa T (2019) Cortical bone response toward nanosecond-pulsed laser-treated zirconia implant surfaces. *Dent Mater J* 38:444–451. <https://doi.org/10.4012/dmj.2018-153>
44. Nassif W, Rifai M (2018) Surface characterization and cell adhesion of different zirconia treatments: an in vitro Study. *J Contemp Dent Pract* 19:181–188. <https://doi.org/10.5005/JP-JOURNALS-10024-2234>
45. Hao L, Lawrence J, Chian KS, Low DKY, Lim GC, Zheng HY (2004) The formation of a hydroxyl bond and the effects thereof on bone-like apatite formation on a magnesia partially stabilized zirconia (MgO-PSZ) bioceramic following CO<sub>2</sub> laser irradiation. *J Mater Sci Mater Med* 15:967–975. <https://doi.org/10.1023/B:JMSM.0000042682.20595.74>
46. Calvo-Guirado JL, Aguilar Salvatierra A, Gargallo-Albiol J, Delgado-Ruiz RA, Maté Sanchez JE, Satorres-Nieto M (2014) Zirconia with laser-modified microgrooved surface vs. titanium implants covered with melatonin stimulates bone formation. Experimental study in tibia rabbits. *Clin Oral Implants Res* 26:1421–1429. <https://doi.org/10.1111/clr.12472>
47. Calvo-Guirado JL, Aguilar-Salvatierra A, Gomez-Moreno G, Guardia J, Delgado-Ruiz RA, Mate-Sanchez de Val JE (2014) Histological, radiological and histomorphometric evaluation of immediate vs. non-immediate loading of a zirconia implant with surface treatment in a dog model. *Clin. Oral Implants Res* 25:826–830. <https://doi.org/10.1111/clr.12145>
48. Glauser R, Sailer I, Wohlwend A, Studer S, Schibli M, Schärer P (2004) Experimental zirconia abutments for implant-supported single-tooth restorations in esthetically demanding regions: 4-year results of a prospective clinical study. *Int J Prosthodont* 17:285–290
49. Kohal RJ, Klaus G (2004) A zirconia implant-crown system: a case report. *Int J Periodontics Restorative Dent* 24:147–153
50. Piconi C, Maccauro G, Muratori F, Brach Del Prever E (2003) Alumina and zirconia ceramics in joint replacements. *J Appl Biomater Biomech* 1:19–32. <https://doi.org/10.1177/228080000300100103>
51. Kohorst P, Borchers L, Stempel J, Stiesch M, Hassel T, Bach FW, Hübsch C (2012) Low-temperature degradation of different zirconia ceramics for dental applications. *Acta biomaterialia* 8(3):1213–1220. <https://doi.org/10.1016/j.actbio.2011.11.016>
52. Taniguchi Y, Kakura K, Yamamoto K, Kido H, Yamazaki J (2015) Accelerated osteogenic differentiation and bone formation on zirconia with surface grooves created with fiber laser irradiation. *Clin Implant Dent Relat Res* 18:883–894. <https://doi.org/10.1111/cid.12366>
53. Hoffmann O, Angelov N, Zafiropoulos G-G, Andreana S (2012) Osseointegration of zirconia implants with different surface characteristics: an evaluation in rabbits. *Int J Oral Maxillofac Implant* 27:352–358
54. Scarano A, Piattelli M, Caputi S, Favero GA, Piattelli A (2004) Bacterial adhesion on titanium nitride-coated and uncoated implants: an in vivo human study. *J Periodontol* 75:292–296. [https://doi.org/10.1563/1548-1336\(2003\)029%3c0080:BAOTNA%3e2.3.CO;2](https://doi.org/10.1563/1548-1336(2003)029%3c0080:BAOTNA%3e2.3.CO;2)
55. Deville S, Chevalier J, Gremillard L (2006) Influence of surface finish and residual stresses on the ageing sensitivity of biomedical grade zirconia. *Biomaterials* 27:2186–2192. <https://doi.org/10.1016/j.biomaterials.2005.11.021>

**Publisher's note** Springer Nature remains neutral with regard to jurisdictional claims in published maps and institutional affiliations.